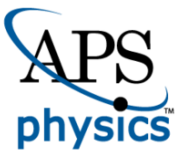

Gravity-driven instability of a thin liquid film underneath a soft solid

S. H. Lee, K. L. Maki, D. Flath, S. J. Weinstein, C. Kealey, W. Li, C. Talbot, and S. Kumar

Phys. Rev. E **90**, 053009 — Published 17 November 2014

DOI: 10.1103/PhysRevE.90.053009

Gravity-driven instability of a thin liquid film underneath a soft solid

S. H. Lee,[=] K. L. Maki,[&] D. Flath,[+] S. J. Weinstein,[#]
C. Kealey,[*] W. Li,[+] C. Talbot,[″] and S. Kumar[=]

[&]School of Mathematical Sciences, Rochester Institute of Technology, Rochester, NY
[+]Department of Mathematics, Statistics, and Computer Science, Macalester College, St. Paul, MN
[#]Department of Chemical Engineering, Rochester Institute of Technology, Rochester, NY
[*]Department of Mathematics, Beloit College, Beloit, WI
[″]Department of Mathematics, University of Connecticut, Storrs, CT
[=]Department of Chemical Engineering and Materials Science, University of Minnesota, Minneapolis, MN

Abstract - The gravity-driven instability of a thin liquid film located underneath a soft solid material is considered. The equations and boundary conditions governing the solid deformation are systematically converted from a Lagrangian representation to an Eulerian representation, which is the natural framework for describing the liquid motion. This systematic conversion reveals that the continuity-of-velocity boundary condition at the liquid-solid interface is more complicated than has previously been assumed, even in the small-strain limit. We then make clear the conditions under which the commonly used simplified version of this boundary condition is valid. The small-strain approximation, lubrication theory, and linear stability analysis are applied to derive an expression for the growth rate of small-amplitude perturbations. Asymptotic analysis reveals that the coupling between the liquid and solid manifests itself as a lower effective liquid-air interfacial tension that leads to larger instability growth rates. Although this suggests that it is more difficult to maintain a stable liquid coating underneath a soft solid, the effect is expected to be weak for cases of practical interest.

1 Introduction

One very challenging class of problems in interfacial fluid mechanics concerns the flow of liquids near deformable solid boundaries. In addition to the strong nonlinearity introduced by the presence of a deformable interface, care must be taken to properly couple the motion of the liquid—typically described from an Eulerian perspective—with that of the solid—typically described from a Lagrangian perspective.

The present paper has two objectives. The first is to present a systematic derivation of the governing equations and boundary conditions that describe the liquid-solid interface. In doing so, we will begin with a Lagrangian description of the solid motion and carefully convert it to an Eulerian description. We will show that even when the displacement gradients are small (the small-strain limit), the continuity-of-velocity boundary condition at the liquid-solid interface is more complicated than has previously been assumed. Our systematic conversion allows us to make clear the conditions under which the commonly used simplified version of this boundary condition is valid.

The second objective of this paper is to study the gravity-driven instability of a thin liquid film underneath a deformable, or soft, solid layer. Although the case where the solid is rigid has been well studied [1], the influence of solid deformability appears not to have been worked out and is of fundamental interest. This problem is also of practical interest since the liquid film may represent a coating and one would like to know whether solid deformability enhances or delays its instability.

In §2 we derive the governing equations and boundary conditions with a focus on the small-strain limit, and obtain further simplifications through application of the lubrication approximation. A linear stability analysis is described in §3, with results presented in §4. Finally, conclusions are given in §5.

2 Governing Equations

We consider a system consisting of an incompressible Newtonian liquid layer lying underneath an incompressible, impermeable, and deformable viscoelastic solid (Fig. 1), which we refer to as a gel. The gel is fixed to a rigid substrate that is horizontal and the liquid layer is in contact with passive air. We focus on two-dimensional disturbances with respect to x and z, where x denotes the horizontal coordinate and z denotes the coordinate normal to the rigid substrate; the system is assumed invariant in the y-direction, which is oriented out of the plane of Fig. 1. The interfaces are initially flat such that the the liquid is in the region $0 \leq z \leq R$, and the gel is in the region $-HR \leq z \leq 0$, where H is a constant.

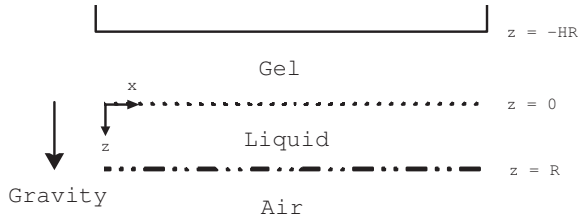

Figure 1: Coordinate system for liquid film lying underneath a deformable solid.

2.1 Liquid Motion

An Eulerian perspective is used to describe the motion of the liquid. The liquid motion is thus governed by:

$$\rho^\ell \left(\frac{\partial \mathbf{v}^\ell}{\partial t} + \mathbf{v}^\ell \cdot \nabla \mathbf{v}^\ell \right) = \nabla \cdot \mathbf{T}^\ell + \rho^\ell g \mathbf{k}, \tag{1}$$

$$\nabla \cdot \mathbf{v}^\ell = 0, \tag{2}$$

where ρ^ℓ is the density of the liquid, $\mathbf{v}^\ell$ is the velocity vector of the liquid, $\mathbf{T}^\ell$ is the stress tensor of the liquid, and g is the gravitational acceleration. The operator $\nabla = \mathbf{i}\,\partial/\partial x + \mathbf{k}\,\partial/\partial z$, where $\mathbf{i}$ and $\mathbf{k}$ denote the unit vectors in the $x-$ and $z-$directions,

respectively. The liquid is modeled as Newtonian so the total stress tensor is given by:

$$\mathbf{T}^{\ell} = -p^{\ell}\mathbf{I} + \eta^{\ell}\left(\nabla\mathbf{v}^{\ell} + \left(\nabla\mathbf{v}^{\ell}\right)^{T}\right), \tag{3}$$

where the pressure is denoted by p^{ℓ}, $\mathbf{I}$ is the identity tensor, η^{ℓ} is the liquid viscosity, and the superscript T denotes transpose. At the liquid-air interface $z = f^{\ell}(x,t)$, we impose a zero-shear-stress condition and set the normal-stress difference across the interface equal to the surface tension, denoted by σ^{a}, times the mean curvature of the interface. In addition, the kinematic condition is applied at this interface.

2.2 Gel Motion

The stress and strain in a solid are most naturally described from a Lagrangian perspective, as the strain invoked is determined via reference to the undeformed locations in the body. However, the motion of the liquid is more naturally described in Eulerian form, where the motion of arbitrary material bodies of finite volume can be tracked in time, and the formalism of continuum mechanics can be applied to generate differential field equations. In addition, the gel and liquid motions are intimately coupled. In what follows, we present general governing equations for the gel from an Eulerian perspective. The stress in the gel is indeed described in Lagrangian form, but then is carefully mapped back to the Eulerian perspective so it can be inserted into the Eulerian equations of motion.

From an Eulerian perspective, the motion of the gel is governed by statements of momentum and mass conservation:

$$\rho^{s}\left(\frac{\partial\mathbf{v^s}}{\partial t} + \mathbf{v^s}\cdot\nabla\mathbf{v^s}\right) = \nabla\cdot\mathbf{T^s} + \rho^{s}g\mathbf{k} \tag{4}$$

$$\nabla\cdot\mathbf{v^s} = 0 \tag{5}$$

where ρ^{s}, $\mathbf{v^s}$, and $\mathbf{T^s}$ are, respectively, the density, velocity vector, and stress tensor of the gel. For simplicity, we adopt the approach of much prior literature and model the gel as a Kelvin-Voigt material. In the Kelvin-Voigt model, the motion of the gel is represented by a viscous damper and purely elastic spring connected in parallel.

Although here we focus on the small-strain limit, we note that accounting for the effect of finite strains in the gel requires the use of a nonlinear constitutive model [2, 3]. Before considering the expression for $\mathbf{T^s}$, we review mass conservation from a Lagrangian perspective; this is necessary to carefully establish conditions under which the approximations used in the analysis to follow are valid.

The dynamics of the gel are characterized by the Lagrangian displacement field, the measurement of the deviation of the gel from its unstressed state. The reference configuration has independent spatial variables (X, Z) to characterize the material particles in the reference (i.e., unstressed) frame. In the deformed state, the (x, z) spatial location of the material particle (X, Z) in the reference configuration is given by:

$$x = X + U_x(X, Z, t) \quad \text{and} \quad z = Z + U_z(X, Z, t), \tag{6}$$

where U_x and U_z are the Lagrangian displacements in the $x-$ and $z-$directions, respectively.

In the limit of small strains, the incompressibility of the gel is expressed as

$$\frac{\partial U_x}{\partial X} + \frac{\partial U_z}{\partial Z} = 0. \tag{7}$$

To see why, we consider an initially rectangular gel element in the $XZ-$plane with sides ΔX and ΔZ aligned with and parallel to the $X-$ and $Z-$axes, respectively. The area of this element is thus $\Delta X \Delta Z$. This rectangle is deformed in the $xz-$plane as shown in Fig. 2 and has vertices given by:

$$\begin{aligned}
P_1 &= (X + U_x(X, Z, t), Z + U_z(X, Z, t)), \\
P_2 &= (X + U_x(X, Z + \Delta Z, t), Z + \Delta Z + U_z(X, Z + \Delta Z, t)), \\
P_3 &= (X + \Delta X + U_x(X + \Delta X, Z + \Delta Z, t), Z + \Delta Z + U_z(X + \Delta X, Z + \Delta Z, t)), \\
P_4 &= (X + \Delta X + U_x(X + \Delta X, Z, t), Z + U_z(X + \Delta X, Z, t)).
\end{aligned}$$

The area of the stretched gel element is given by the cross product $|\mathbf{P_1P_2} \times \mathbf{P_1P_4}|$. If we ignore quadratic terms in the Taylor expansions as ΔX and ΔZ approach zero, then the vectors $\mathbf{P_1P_2}$ and $\mathbf{P_1P_4}$ are given by:

$$\begin{aligned}
\mathbf{P_1P_2} &= \left(\Delta Z \frac{\partial U_x}{\partial Z}(X, Z, t), \Delta Z + \Delta Z \frac{\partial U_z}{\partial Z}(X, Z, t) \right), \\
\mathbf{P_1P_4} &= \left(\Delta X + \Delta X \frac{\partial U_x}{\partial Z}(X, Z, t), \Delta X \frac{\partial U_z}{\partial X}(X, Z, t) \right).
\end{aligned}$$

Thus, the area of the stretched gel element is

$$\left|\frac{\partial U_x}{\partial Z}\frac{\partial U_z}{\partial X} - \left(1+\frac{\partial U_z}{\partial Z}\right)\left(1+\frac{\partial U_x}{\partial X}\right)\right| \Delta X \Delta Z. \tag{8}$$

For the volume to be conserved, i.e., the area remains as $\Delta X \Delta Z$, we must have

$$\frac{\partial U_z}{\partial Z} + \frac{\partial U_x}{\partial X} + \frac{\partial U_z}{\partial Z}\frac{\partial U_x}{\partial X} - \frac{\partial U_x}{\partial Z}\frac{\partial U_z}{\partial X} = 0. \tag{9}$$

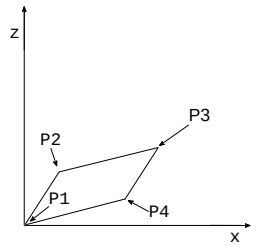

Figure 2: Stretched gel element in the xz-plane.

In this work, we will apply the small-strain approximation, which requires that the displacement gradients be small compared to unity, i.e.,

$$\frac{\partial U_x}{\partial X} << 1, \quad \frac{\partial U_x}{\partial Z} << 1, \quad \frac{\partial U_z}{\partial X} << 1, \quad \text{and} \quad \frac{\partial U_z}{\partial Z} << 1. \tag{10}$$

This approximation allows products of displacement gradients to be dropped from (9) and leads to the incompressibility condition stated in (7).

The strain, or measure of deformation in the gel, is given by spatial derivatives of the displacement fields. The components of the resulting Lagrangian infinitesimal-strain tensor $\mathbf{L}$ are given by:

$$L_{xx} = \frac{\partial U_x}{\partial X},\ L_{xz} = L_{zx} = \frac{1}{2}\left(\frac{\partial U_x}{\partial Z} + \frac{\partial U_z}{\partial X}\right),\ \text{and}\ L_{zz} = \frac{\partial U_z}{\partial Z}. \tag{11}$$

To characterize the purely elastic behavior, we use Hooke's law for an isotropic medium. For an incompressible solid subject to (7), the elastic stress $\mathbf{T^E}$ is

$$\mathbf{T^E} = 2E\mathbf{L}, \tag{12}$$

where E is the shear modulus.

The velocity field in the gel is the time derivative of the position (6):

$$\frac{dx}{dt} = \frac{\partial U_x}{\partial t} \text{ and } \frac{dz}{dt} = \frac{\partial U_z}{\partial t}, \tag{13}$$

since X and Z are independent of time. Therefore, the rate-of-strain tensor is given by $\partial \mathbf{L}/\partial t$ and the viscous stress $\mathbf{T^V}$ is characterized by:

$$\mathbf{T^V} = 2\eta^s \frac{\partial \mathbf{L}}{\partial t}, \tag{14}$$

where η^s is the viscosity of the gel. The total stress tensor in the gel, in accordance with the assumed Kelvin-Voigt model, is

$$\mathbf{T^s} = -P^s\mathbf{I} + \mathbf{T^V} + \mathbf{T^E}, \tag{15}$$

where P^s denotes the pressure in the gel, and is the desired stress tensor to be used in conjunction with (4). The constitutive law is linear from the Lagrangian perspective.

A complication in using (4) is that the total stress tensor, $\mathbf{T^s}$, is expressed in Lagrangian coordinates X and Z, and this needs to be converted to Eulerian coordinates x and z to be used. To do so, we introduce the Eulerian displacements u_x and u_z satisfying the equations

$$x = X + u_x(x, z, t) \qquad \text{and} \qquad z = Z + u_z(x, z, t),$$

as well as an Eulerian pressure p^s. When (X, Z, t) and (x, z, t) correspond, in the sense that at time t the material particle (X, Z) is at physical location (x, z), we have

$$U_x(X, Z, t) = u_x(x, z, t), \quad U_z(X, Z, t) = u_z(x, z, t) \text{ and } P^s(X, Z, t) = p^s(x, z, t).$$

More formally, we have by definition:

$$\begin{aligned} U_x(X, Z, t) &= u_x(X + U_x(X, Z, t), Z + U_z(X, Z, t), t), \\ U_z(X, Z, t) &= u_z(X + U_x(X, Z, t), Z + U_z(X, Z, t), t), \\ P^s(X, Z, t) &= p^s(X + U_x(X, Z, t), Z + U_z(X, Z, t), t). \end{aligned}$$

Physically, the Lagrangian description fixes attention on specific particles of the gel, whereas the Eulerian description concerns itself with a particular region of the space occupied by the gel.

To write down general formulas mapping the Lagrangian derivatives into Eulerian derivatives, we assume we have a generic function with $H(X,Z,t) = h(x(X,Z,t), z(X,Z,t), t)$. Using the relationships $x = X + U_x(X,Z,t)$ and $z = Z + U_z(X,Z,t)$, we find:

$$\left.\frac{\partial H}{\partial X}\right|_{Z,t} = \left.\frac{\partial h}{\partial x}\right|_{z,t}\left(1 + \left.\frac{\partial U_x}{\partial X}\right|_{Z,t}\right) + \left.\frac{\partial h}{\partial z}\right|_{x,t}\left(\left.\frac{\partial U_z}{\partial X}\right|_{Z,t}\right), \tag{16}$$

where the subscript indicates what independent variables are being held fixed when derivatives are taken. To generate equations for the Lagrangian partial derivatives of U_x and U_z in terms of Eulerian partial derivatives of u_x and u_z, we use the generic formula (16) with $H = U_x$ and $h = u_x$ as well as $H = U_z$ and $h = u_z$. We find:

$$\left.\frac{\partial U_x}{\partial X}\right|_{Z,t} = \frac{A}{J}, \quad \left.\frac{\partial U_z}{\partial X}\right|_{Z,t} = \frac{B}{J}, \text{ where} \tag{17}$$

$$\begin{aligned} A &= \left.\frac{\partial u_x}{\partial x}\right|_{z,t} - \left.\frac{\partial u_x}{\partial x}\right|_{z,t}\left.\frac{\partial u_z}{\partial z}\right|_{x,t} + \left.\frac{\partial u_x}{\partial z}\right|_{x,t}\left.\frac{\partial u_z}{\partial x}\right|_{z,t}, \\ B &= \left.\frac{\partial u_z}{\partial x}\right|_{z,t}, \\ J &= 1 - \left.\frac{\partial u_x}{\partial x}\right|_{z,t} - \left.\frac{\partial u_z}{\partial z}\right|_{x,t} + \left.\frac{\partial u_x}{\partial x}\right|_{z,t}\left.\frac{\partial u_z}{\partial z}\right|_{x,t} - \left.\frac{\partial u_x}{\partial z}\right|_{x,t}\left.\frac{\partial u_z}{\partial x}\right|_{z,t}. \end{aligned}$$

An identical process is used to map the partial derivatives with respect to Z:

$$\left.\frac{\partial U_x}{\partial Z}\right|_{X,t} = \frac{C}{J}, \quad \left.\frac{\partial U_z}{\partial Z}\right|_{X,t} = \frac{D}{J}, \text{ where} \tag{18}$$

$$\begin{aligned} C &= \left.\frac{\partial u_x}{\partial z}\right|_{x,t}, \\ D &= \left.\frac{\partial u_z}{\partial z}\right|_{x,t} - \left.\frac{\partial u_x}{\partial x}\right|_{z,t}\left.\frac{\partial u_z}{\partial z}\right|_{x,t} + \left.\frac{\partial u_x}{\partial z}\right|_{x,t}\left.\frac{\partial u_z}{\partial x}\right|_{z,t}. \end{aligned}$$

We will now formally argue that the small-strain approximation in the Lagrangian coordinates implies the small-strain approximation in the Eulerian coordinates. To

do so, we assume that terms quadratic in the Eulerian derivatives are small and utilize the method of dominant balance. With this assumption, we obtain:

$$\left.\frac{\partial u_x}{\partial x}\right|_{z,t} \sim \left.\frac{\partial U_x}{\partial X}\right|_{Z,t}, \qquad \left.\frac{\partial u_z}{\partial x}\right|_{z,t} \sim \left.\frac{\partial U_z}{\partial X}\right|_{Z,t}, \tag{19}$$

$$\left.\frac{\partial u_x}{\partial z}\right|_{x,t} \sim \left.\frac{\partial U_x}{\partial Z}\right|_{X,t}, \qquad \left.\frac{\partial u_z}{\partial z}\right|_{x,t} \sim \left.\frac{\partial U_z}{\partial Z}\right|_{X,t}. \tag{20}$$

Substituting these results back into (17) and (18), and invoking incompressibility of the gel (7) in J (defined in (17)) shows that indeed quadratic terms in the Eulerian derivatives are equivalent in order to quadratic terms in the Lagrangian derivatives. Thus, equations (19) and (20) are asymptotically consistent with the small-strain approximation used in the Lagrangian framework.

Next, we determine the consequence of the infinitesimal-strain approximation on the time derivatives. Specifically, we again assume we have a generic function with $H(X,Z,t) = h(x(X,Z,t), z(X,Z,t), t)$. Using the relationships $x = X + U_x(X,Z,t)$ and $z = Z + U_z(X,Z,t)$, we find:

$$\left.\frac{\partial H}{\partial t}\right|_{X,Z} = \left.\frac{\partial h}{\partial x}\right|_{z,t}\left(\left.\frac{\partial U_x}{\partial t}\right|_{X,Z}\right) + \left.\frac{\partial h}{\partial z}\right|_{x,t}\left(\left.\frac{\partial U_z}{\partial t}\right|_{X,Z}\right) + \left.\frac{\partial h}{\partial t}\right|_{x,z}. \tag{21}$$

To generate Lagrangian time derivatives of U_x and U_z in terms of Eulerian partial derivatives of u_x and u_z, we use the generic formula (21) with $H = U_x$ and $h = u_x$ as well as $H = U_z$ and $h = u_z$. We find:

$$\left.\frac{\partial U_x}{\partial t}\right|_{X,Z} = \frac{\alpha}{J}, \quad \left.\frac{\partial U_z}{\partial t}\right|_{X,Z} = \frac{\gamma}{J}, \text{ where} \tag{22}$$

$$\alpha = \left.\frac{\partial u_x}{\partial t}\right|_{x,z} - \left.\frac{\partial u_x}{\partial t}\right|_{x,z}\left.\frac{\partial u_z}{\partial z}\right|_{x,t} + \left.\frac{\partial u_x}{\partial z}\right|_{x,t}\left.\frac{\partial u_z}{\partial t}\right|_{x,z},$$

$$\gamma = \left.\frac{\partial u_z}{\partial t}\right|_{x,z} - \left.\frac{\partial u_z}{\partial t}\right|_{x,z}\left.\frac{\partial u_x}{\partial x}\right|_{z,t} + \left.\frac{\partial u_z}{\partial x}\right|_{z,t}\left.\frac{\partial u_x}{\partial t}\right|_{x,z},$$

and J is again given in (17). Using the small-strain approximation, (19) and (20), and the incompressibility of the gel (7), we obtain:

$$\left.\frac{\partial U_x}{\partial t}\right|_{X,Z} \sim \left.\frac{\partial u_x}{\partial t}\right|_{x,z} - \left.\frac{\partial u_x}{\partial t}\right|_{x,z}\left.\frac{\partial u_z}{\partial z}\right|_{x,t} + \left.\frac{\partial u_x}{\partial z}\right|_{x,t}\left.\frac{\partial u_z}{\partial t}\right|_{x,z}, \tag{23}$$

$$\left.\frac{\partial U_z}{\partial t}\right|_{X,Z} \sim \left.\frac{\partial u_z}{\partial t}\right|_{x,z} - \left.\frac{\partial u_z}{\partial t}\right|_{x,z}\left.\frac{\partial u_x}{\partial x}\right|_{z,t} + \left.\frac{\partial u_z}{\partial x}\right|_{z,t}\left.\frac{\partial u_x}{\partial t}\right|_{x,z}. \tag{24}$$

Note that in (23) and (24), terms involving products of a displacement gradient and a time derivative cannot generally be neglected, even in spite of the fact that the small-strain limit has already been invoked. Nevertheless, prior works (e.g., [4]-[8]) have neglected these terms, apparently without realizing it. However, we can now make clear the conditions under which the commonly used simplified version of these equations is valid.

Equations (23) and (24) can be greatly simplified by considering the following order-of-magnitude argument. In the small-strain limit, $u_x, u_z \sim \delta$ and $x, z \sim L$ such that $\delta/L \ll 1$ where δ is a characteristic displacement and L is length scale characteristic of the problem geometry. Suppose that $t \sim L/U$ where U is a characteristic velocity. Then, the time derivative terms are $O(\delta U/L)$, and the terms involving products of a time derivative and displacement gradient are an order of magnitude smaller. This implies:

$$\left.\frac{\partial u_x}{\partial t}\right|_{x,z} \sim \left.\frac{\partial U_x}{\partial t}\right|_{X,Z}, \tag{25}$$

$$\left.\frac{\partial u_z}{\partial t}\right|_{x,z} \sim \left.\frac{\partial U_z}{\partial t}\right|_{X,Z}. \tag{26}$$

Thus, when prior works use (25) and (26) they implicitly assume the above scalings.

The assumptions of lubrication theory, which we will apply later, are consistent with the above order-of-magnitude argument. However, even within the small-strain limit there could conceivably be regimes where this argument does not hold, e.g., if $t \sim \delta/U$, this corresponds to much faster motions than those considered above. This is an important point that appears to have been overlooked in prior work, but becomes clear through a systematic conversion from a Lagrangian framework to an Eulerian one.

With the above results, the components of the Eulerian total stress tensor are given by:

$$\mathbf{T}^{\mathbf{s}}_{xx} = -p^s + 2\eta^s \frac{\partial v_x^s}{\partial x} + 2E\frac{\partial u_x}{\partial x}, \tag{27}$$

$$\mathbf{T}^{\mathbf{s}}_{xz} = \mathbf{T}^{\mathbf{s}}_{zx} = \eta^s \left(\frac{\partial v_x^s}{\partial z} + \frac{\partial v_z^s}{\partial x}\right) + E\left(\frac{\partial u_x}{\partial z} + \frac{\partial u_z}{\partial x}\right), \tag{28}$$

$$\mathbf{T}^{\mathbf{s}}_{zz} = -p^s + 2\eta^s \frac{\partial v_z^s}{\partial z} + 2E\frac{\partial u_z}{\partial z}, \tag{29}$$

where

$$v_x^s = \frac{\partial u_x}{\partial t}, \tag{30}$$

$$v_z^s = \frac{\partial u_z}{\partial t}. \tag{31}$$

(The expressions for v_x^s and v_z^s from a Lagrangian perspective are given by (13).) Here, the constitutive law is linear from an Eulerian perspective, but it would have been nonlinear had the terms in (23) and (24) involving products of a displacement gradient and a time derivative been retained. In addition, we note that (30) and (31) are the expressions used in prior work, where they are simply written down (e.g., [4]-[8]). However, the order-of-magnitude arguments given above make clear the assumptions under which these expressions are valid.

We now state the remaining boundary conditions. At the rigid plane $z = -HR$, the displacements are zero; that is, the deformable gel is perfectly attached to the horizontal plane. At the gel-liquid interface, $z = f^s(x,t)$, the normal and tangential stresses in the gel and liquid are balanced:

$$\mathbf{n^s} \cdot \mathbf{T}^\ell - \mathbf{n^s} \cdot \mathbf{T^s} + 2\sigma^s \mathcal{H} \mathbf{n^s} = 0, \tag{32}$$

where $\mathbf{n^s}$ is the normal vector to the gel-liquid interface that points into the liquid, σ^s is the surface tension of the gel-liquid interface, and $\mathcal{H}$ is the mean curvature of the gel-liquid interface. The velocities in the gel and the liquid are equal, which enforces both the no-slip and no-penetration conditions,

$$v_x^s = v_x^\ell \quad \text{and} \quad v_z^s = v_z^\ell. \tag{33}$$

In addition, there is a kinematic condition describing the location of the gel-liquid interface. In what follows, we simplify the calculations by studying the limit in which the gel has no viscosity. Thus, $\eta^s = 0$ and we refer to the gel as a solid.

2.3 Leading-Order Equations

The liquid thickness R is taken as a characteristic length scale in the vertical direction. We denote the characteristic length scale in the horizontal direction as λ and assume that $\epsilon = R/\lambda \ll 1$, allowing us to focus on long-wavelength perturbations to the system [1, 9]. Specific choices could be made for λ (e.g., the instability wavelength), but here we leave λ arbitrary for generality. The governing equations are made dimensionless with the following scalings:

$$x' = \frac{x}{\lambda}, \quad z' = \frac{z}{\epsilon\lambda}, \quad t' = \frac{t}{\lambda/V}, \tag{34}$$

$$(v_x^\ell)' = \frac{v_x^\ell}{V}, \quad (v_z^\ell)' = \frac{v_z^\ell}{\epsilon V}, \quad (p^\ell)' = \frac{p^\ell}{\eta^\ell V/(\epsilon^2\lambda)}, \tag{35}$$

$$u_x' = \frac{u_x}{\lambda}, \quad u_z' = \frac{u_z}{\epsilon\lambda}, \quad (p^s)' = \frac{p^s}{\eta^\ell V/(\epsilon^2\lambda)}, \tag{36}$$

where V is a characteristic velocity scale in the x-direction. Note that the scaling of time is consistent with the order-of-magnitude argument given in the previous section. It should also be recognized that in order to be consistent with both the small-strain limit and lubrication theory, we require $\delta/R \ll 1$ and $R/\lambda \ll 1$, where δ is a characteristic displacement.

In the limit $\epsilon \to 0$, the following leading-order dimensionless equations are obtained in the liquid:

$$0 = -\frac{\partial p^\ell}{\partial x} + \frac{\partial^2 v_x^\ell}{\partial z^2}, \tag{37}$$

$$0 = -\frac{\partial p^\ell}{\partial z} + \epsilon G, \tag{38}$$

$$0 = \frac{\partial v_x^\ell}{\partial x} + \frac{\partial v_z^\ell}{\partial z}, \tag{39}$$

where $G = \rho^\ell g R^2/\eta^\ell V$ reflects the physical balance between the gravitational and viscous forces (from the liquid). We note that one could define a rescaled version of G equal to ϵG if desired. At the liquid-air interface $z = f^\ell(x,t)$, we have:

$$\frac{\partial f^\ell}{\partial t} + v_x^\ell \frac{\partial f^\ell}{\partial x} = v_z^\ell, \tag{40}$$

$$p^a - p^\ell = S^a \frac{\partial^2 f^\ell}{\partial x^2}, \tag{41}$$

$$\frac{\partial v_x^\ell}{\partial z} = 0, \tag{42}$$

where $S^a = \epsilon^3\sigma^a/\eta^\ell V$ is the ratio of the forces due to the liquid-air interfacial tension relative to those due to the liquid viscosity, and p^a is the pressure of the air, taken to be zero.

In the solid, we have:

$$-\frac{\partial p^s}{\partial x} + \bar{E}\frac{\partial^2 u_x}{\partial z^2} = 0, \tag{43}$$

$$-\frac{\partial p^s}{\partial z} + \epsilon\rho G = 0, \tag{44}$$

$$\frac{\partial u_x}{\partial x} + \frac{\partial u_z}{\partial z} = 0, \tag{45}$$

where $\bar{E} = E\lambda/\eta^\ell V$ measures the relative significance of elastic to viscous forces (from the liquid), and $\rho = \rho^s/\rho^\ell$ is the solid-liquid density ratio. At the surface of the horizontal plane $z = -H$,

$$u_x(x, -H, t) = 0 \quad \text{and} \quad u_z(x, -H, t) = 0. \tag{46}$$

Finally, at the liquid-solid interface $z = f^s(x, t)$, the kinematic condition, continuity-of-velocity boundary conditions, and continuity-of-stress boundary conditions become

$$\frac{\partial f^s}{\partial t} + v_x^\ell\frac{\partial f^s}{\partial x} = v_z^\ell, \tag{47}$$

$$\frac{\partial u_x}{\partial t} = v_x^\ell, \tag{48}$$

$$\frac{\partial u_z}{\partial t} = v_z^\ell, \tag{49}$$

$$p^\ell - p^s = S^s\frac{\partial^2 f^s}{\partial x^2}, \tag{50}$$

$$\frac{\partial v_x^\ell}{\partial z} = \bar{E}\frac{\partial u_x}{\partial z}, \tag{51}$$

where $S^s = \epsilon^3\sigma^s/\eta^\ell V$ is the ratio of the forces due to the gel-liquid interfacial tension relative to those due to the liquid viscosity.

3 Linear Stability Analysis

The base state of the present system corresponds to flat liquid-solid and liquid-air interfaces that are located at $z = 0$ and $z = 1$, respectively. The liquid is at rest and

the solid is undeformed in the base state. The velocity and pressure distributions in the base state, denoted by an overbar, are solutions to the leading-order system (37)-(51) with no free-surface or interfacial deformations ($\bar{f}^s = 0$ and $\bar{f}^\ell = 1$):

$$\bar{v}_x^\ell = 0, \quad \bar{v}_z^\ell = 0, \text{ and } \bar{p}^\ell = \epsilon G(z-1). \tag{52}$$

The base-state displacements in the solid are

$$\bar{u}_x = 0, \quad \bar{u}_z = 0, \text{ and } \bar{p}^s = \epsilon G(\rho z - 1). \tag{53}$$

We study the stability of the base state to small-amplitude perturbations. To each variable, a perturbation of the form

$$F'(x,z,t) = \tilde{F}(z) e^{i(kx-\omega t)}, \tag{54}$$

where $\tilde{F}(z)$ is a complex-valued eigenfunction, k is a wavenumber, and ω is a complex-valued growth rate, is added to the base state and substituted into the leading-order system. With this choice for the normal mode, the perturbation quantities grow and instability occurs when the imaginary part of ω, denoted by $\mathrm{Im}\,[\omega]$, is positive. Note that the quantities and $f^\ell(x,t)$ and $f^s(x,t)$ do not depend on z, so the quantities $\tilde{f}^\ell$ and $\tilde{f}^s$ are constants.

The governing equations for the perturbation quantities in the liquid and the solid, respectively, are given by:

$$0 = -ik\tilde{p}^\ell + \frac{d^2\tilde{v}_x^\ell}{dz^2}, \tag{55}$$

$$0 = -\frac{d\tilde{p}^\ell}{dz}, \tag{56}$$

$$0 = ik\tilde{v}_x^\ell + \frac{d\tilde{v}_z^\ell}{dz}, \tag{57}$$

$$0 = -ik\tilde{p}^s + \bar{E}\frac{d^2\tilde{u}_x}{dz^2}, \tag{58}$$

$$0 = -\frac{d\tilde{p}^s}{dz}, \tag{59}$$

$$0 = ik\tilde{u}_x + \frac{d\tilde{u}_z}{dz}. \tag{60}$$

At the liquid-air interface, $z = 1$, we apply a domain perturbation method to find

$$-i\omega\tilde{f}^{\ell} = \tilde{v}_z^{\ell}, \tag{61}$$

$$-\epsilon G\tilde{f}^{\ell} - \tilde{p}^{\ell} = -k^2 S^a \tilde{f}^{\ell}, \tag{62}$$

$$\frac{d\tilde{v}_x^{\ell}}{dz} = 0, \tag{63}$$

where the first equation is the kinematic condition, the second is the normal force balance, and the third is the tangential force balance. The domain perturbation method involves replacing each variable as the sum of its base state value and a perturbation of the form (54). The boundary conditions are then expanded in a Taylor series around the location of the unperturbed interface and only terms linear in the perturbation quantities are retained [10]. Note that the perturbation parameter associated with the liquid-air interface, $\tilde{f}^{\ell}$, is a constant.

Similarly, at the liquid-solid interface, $z = 0$, the domain perturbation method gives the following five boundary conditions:

$$-i\omega\tilde{f}^{s} = \tilde{v}_z^{\ell}, \tag{64}$$

$$(1-\rho)\epsilon G\tilde{f}^{s} + \tilde{p}^{\ell} - \tilde{p}^{s} = -k^2 S^s \tilde{f}^{s}, \tag{65}$$

$$\frac{d\tilde{v}_x^{\ell}}{dz} = \bar{E}\frac{d\tilde{u}_x}{dz}, \tag{66}$$

$$-i\omega\tilde{u}_x = \tilde{v}_x^{\ell}, \tag{67}$$

$$-i\omega\tilde{u}_z = \tilde{v}_z^{\ell}, \tag{68}$$

where the first equation is the kinematic condition, the second two equations are the force balances, and the final two equations are the continuity-of-velocity boundary conditions in the $x-$ and $z-$directions, respectively. Again, the perturbation parameter associated with the liquid-air interface, $\tilde{f}^{s}$, is a constant in the system above. Finally, to close the system,

$$\tilde{u}_x(-H) = \tilde{u}_z(-H) = 0, \tag{69}$$

at the rigid substrate. The system (55)-(69) constitutes the generalized eigenvalue problem that needs to be solved to complete the linear stability analysis.

The stability problem is solved analytically. From the governing equations for the liquid perturbation quantities, we have:

$$\tilde{v}_x^\ell(z) = \frac{ik\tilde{p}^\ell}{2}z^2 + c_1 z + c_2 \tag{70}$$

$$\tilde{v}_z^\ell(z) = \frac{k^2\tilde{p}^\ell}{6}z^3 - \frac{ikc_1}{2}z^2 - ikc_2 z + c_3, \tag{71}$$

where $\tilde{p}^\ell$, c_1, c_2, and c_3 are constants. Applying the kinematic condition (61), we find:

$$c_3 = -i\omega\tilde{f}^\ell - \frac{k^2\tilde{p}^\ell}{6} + \frac{ikc_1}{2} + ikc_2. \tag{72}$$

The tangential stress condition (63) gives

$$c_1 = -ik\tilde{p}^\ell, \tag{73}$$

and the normal stress condition (62) yields

$$\tilde{p}^\ell = \tilde{f}^\ell(k^2 S^a - \epsilon G). \tag{74}$$

Therefore, the perturbation liquid velocities are given by:

$$\tilde{v}_x^\ell(z) = \frac{ik\tilde{p}^\ell}{2}z^2 - ik\tilde{p}^\ell z + c_2, \tag{75}$$

$$\tilde{v}_z^\ell(z) = \frac{k^2\tilde{p}^\ell}{6}(z^3-1) + \frac{k^2\tilde{p}^\ell}{2}(1-z^2) + ikc_2(1-z) - i\omega\tilde{f}^\ell, \tag{76}$$

where $\tilde{p}^\ell$ is given by equation (74); these velocities are expressed in terms of unknown constants c_2 and $\tilde{f}^\ell$. Similarly, the perturbation quantities for the displacements in the solid are given by

$$\tilde{u}_x(z) = \frac{ik\tilde{p}^s}{\bar{E}}\left(\frac{z^2}{2} - \frac{H^2}{2}\right) + c_4'(z+H), \tag{77}$$

$$\tilde{u}_z(z) = \frac{k^2\tilde{p}^s}{\bar{E}}\left(\frac{z^3}{6} - \frac{H^2 z}{2} - \frac{H^3}{3}\right) - ikc_4'\left(\frac{z^2}{2} + Hz + \frac{H^2}{2}\right), \tag{78}$$

where $\tilde{p}^s$ and c_4' are unknown constants.

We substitute the calculated perturbation quantities into the five liquid-solid boundary conditions (64)-(68) to obtain a linear system of equations for the unknown constants c_2, $\tilde{f}^\ell$, $\tilde{f}^s$, $\tilde{p}^s$, and c_4'. The determinant of the linear system must be zero because we seek nontrivial solutions. The characteristic equation is a quadratic in the complex growth rate, where one root is found to always be zero. The imaginary part of the second root is examined to determine stability.

4 Results

The characteristic equation governing the growth rate is

$$\left[-k^2\frac{H^3}{3}(D1+D2)-k^2H^2(D1)-k^2H(D1)-k^4\frac{H^4}{12\bar{E}}(D1)(D2)-\bar{E}\right]\omega^2 + \left[-k^4\frac{H^3}{9}(D1)(D2)-k^2\frac{1}{3}\bar{E}(D1)\right]i\omega=0, \quad (79)$$

where

$$\begin{aligned} D1 &= k^2S^a-\epsilon G, \\ D2 &= k^2S^s+(1-\rho)\epsilon G. \end{aligned}$$

To further simplify matters, we set $\rho=1$ (the density of the liquid equals the density of the solid) and $S^s=0$ (there is no surface tension at the liquid-solid interface). Then, the non-zero root of the characteristic equation is

$$\omega=-i\frac{-k^2\frac{1}{3}\bar{E}(k^2S^a-\epsilon G)}{-k^2\frac{H^3}{3}(k^2S^a-\epsilon G)-k^2H^2(k^2S^a-\epsilon G)-k^2H(k^2S^a-\epsilon G)-\bar{E}}. \quad (80)$$

Note that in the case where $H=0$ (solid thickness is zero),

$$\mathrm{Im}[\omega]=-k^2\frac{1}{3}(k^2S^a-\epsilon G), \quad (81)$$

which is the well-known result for the case where the solid is rigid [1].

Figure 3 shows how $\mathrm{Im}[\omega]$ varies as function of k, G, and H. Fig. 3(a) shows that the maximum growth rate and the range of unstable wavenumbers increase as G increases. Explicit expressions for the cut-off and most-dangerous wavenumbers are readily obtained,

$$k_{c_{full}}=\sqrt{\frac{\epsilon G}{S^a}} \quad (82)$$

$$k_{m_{full}}=\sqrt{\frac{\epsilon G}{2S^a}} \quad (83)$$

(a)

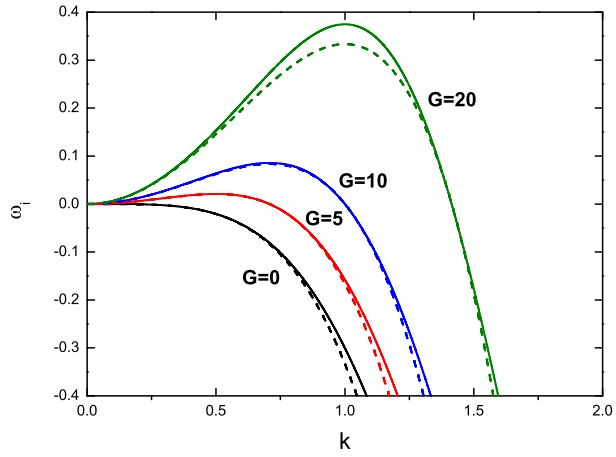

(b)

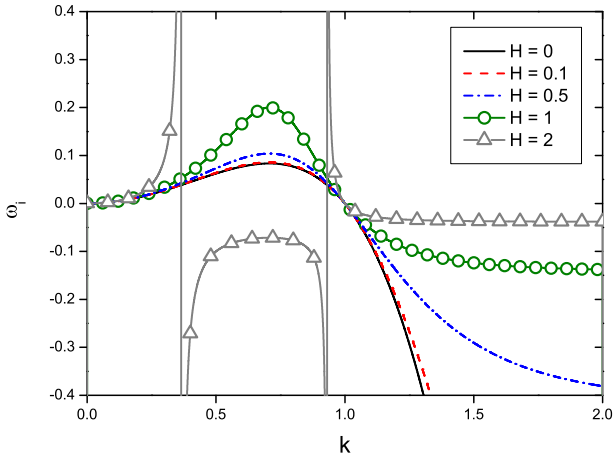

Figure 3: (Color online) (a) Growth rate versus wavenumber for $H = 0$ (dashed line) and $H = 0.1$ (solid line) with $\bar{E} = 1$, $S^a = 1$, $S^s = 0$, $\epsilon = 0.1$, and $\rho = 1$. The case $H = 0$ corresponds to a rigid substrate. (b) Growth rate versus wavenumber for $\bar{E} = 1$, $G = 10$, $S^a = 1$, $S^s = 0$, $\epsilon = 0.1$, $\rho = 1$, and different values of H: $H = 0$ (solid line), $H = 0.1$ (dashed line), $H = 0.5$ (dashed-dot line), $H = 1$ (circles), and $H = 2$ (triangles).

(a)

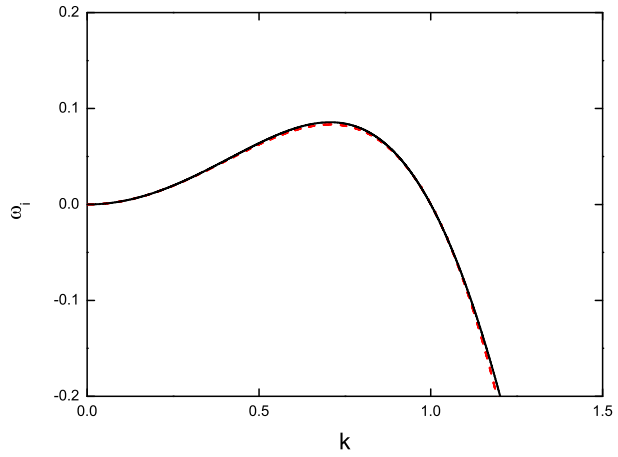

(b)

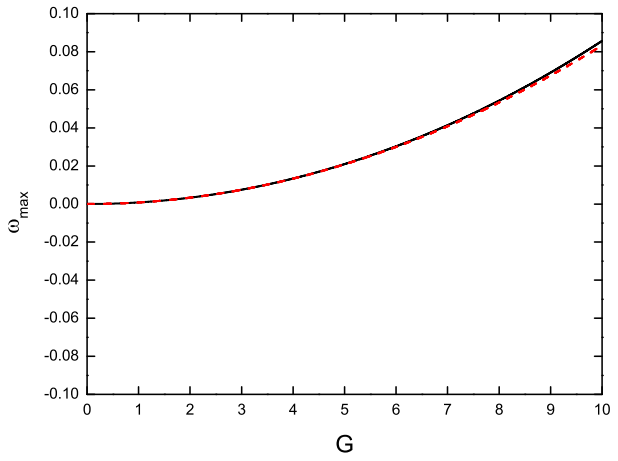

Figure 4: (Color online) (a) Growth rate versus wavenumber for $\bar{E} = 1$, $G = 10$, $H = 0.1$, $S^a = 1$, $S^s = 0$, $\epsilon = 0.1$, and $\rho = 1$: Full equation (solid line), Asymptotic equation (dashed line). (b) Maximum growth rate versus ratio of gravitational to viscous forces for $\bar{E} = 1$, $H = 0.1$, $S^a = 1$, $S^s = 0$, $\epsilon = 0.1$, and $\rho = 1$: Full equation (solid line), Asymptotic equation (dashed line).

These expressions do not depend on the thickness of the deformable layer. We note that setting the value of S^a determines the velocity scale V, and our choice of $S^a = 1$ is consistent with lubrication theory [1, 9].

The maximum growth rate is

$$\mathrm{Im}[\omega]_{m_{full}} = -\frac{\frac{1}{12S^a}\bar{E}(\epsilon^2 G^2)}{\frac{H^3}{12S^a}(\epsilon^2 G^2) + \frac{H^2}{4S^a}(\epsilon^2 G^2) + \frac{H}{4S^a}(\epsilon^2 G^2) - \bar{E}} \tag{84}$$

The maximum growth rate increases when the solid layer is deformable ($H \neq 0$). These features are clearly seen in Fig 3(a). In Fig. 3(b), we see that when $H > 1.35$, the growth rate becomes unbounded at two wavenumbers due to a zero value in the denominator of equation (84). This singularity could be removed by considering inertial terms, but for values of $H < 1.35$ the inertialess theory is expected to yield accurate results [11].

The growth rate can be examined in the limit of small H by performing a Taylor series expansion of (80):

$$\mathrm{Im}[\omega]_{asym.} = -k^2\frac{1}{3}(k^2 S^a - \epsilon G) + k^2\frac{H}{3\bar{E}}k^2(k^2 S^a - \epsilon G)^2 + O(H^2). \tag{85}$$

The leading order term is the expression for a rigid substrate. The $O(H)$ term $\sim k^4$ and is positive, indicating that the coupling between the liquid and solid manifests itself as an lower effective liquid-air interfacial tension. The effect becomes more pronounced for thicker (larger H) and softer (lower $\bar{E}$) solid layers.

In the limit of small H, the maximum growth rate is given by:

$$\mathrm{Im}[\omega]_{m_{asym.}} \approx \frac{1}{3}\left(\frac{\epsilon G}{2}\right)^2\frac{1}{S^a} + \frac{H}{3\bar{E}}\left(\frac{\epsilon G}{2}\right)^4\left(\frac{1}{S^a}\right)^2 + O(H^2). \tag{86}$$

The expressions for the cutoff and most-dangerous wavenumber are the same as (82) and (83). Figure 4 shows that our asymptotic results agree well with predictions from the full equations when $H = 0.1$. Although not shown, we have found good agreement even when $H = 1$ provided that G is sufficiently small. This can be rationalized by noting that the entire $O(H)$ term in (86) can be small even when $H = 1$ provided that the other parameters have suitable values.

Finally, it worthwhile to consider the magnitude of the effect predicted above. If we take $\eta^l = 10^{-3}$ Pa s, $\sigma^l = 0.01$ N/m, $\rho^l = 10^3$ kg/m^3, $E = 100$ Pa, and $\epsilon = 0.1$, then for $G = 10$ and $S_a = 1$ we find $R \sim 100$ μm and $\bar{E} \sim 10^4$. The large value of $\bar{E}$ indicates that even for very soft solids ($E \sim 100$ Pa), the enhancement of the growth rate due to solid deformability is expected to be weak for cases of practical interest. Nevertheless, without carrying out the analysis here, it would not have been obvious to determine whether solid deformability enhances or delays the film instability, and the manner in which it does so (cf. (85)). It is also interesting to note that much stronger effects of solid deformability on liquid behavior have been observed experimentally in cases where the liquid is flowing (e.g., shear flow past a gel) [12]-[14]. In these cases, solid deformability can introduce new instabilities as well as modify existing ones.

5 Conclusions

Systematic conversion of the equations and boundary conditions governing solid deformation reveals that the continuity-of-velocity boundary condition at the liquid-solid interface is more complicated than has previously been assumed, even in the small-strain limit. Terms involving products of a displacement gradient and a time derivative appear and cannot be neglected in the small-strain limit unless the characteristic time scale is $O(L/U)$, where L and U are a characteristic length and velocity, respectively, in the lateral direction. The approach taken here thus makes clear the conditions under which the commonly used simplified version of the continuity-of-velocity boundary condition is valid.

The small-strain approximation, lubrication theory, and linear stability analysis are then applied to study the gravity-driven instability of a liquid film underneath a soft solid. Asymptotic analysis reveals that the coupling between the liquid and solid manifests itself as a lower effective liquid-air interfacial tension that leads to larger instability growth rates. Although this effect is expected to be weak for cases of practical interest, our work is limited to the linear regime and much stronger effects may take place in the nonlinear regime. The systematic approach taken here

provides a framework that could be extended to study nonlinear effects, e.g., through the development of long-wave evolution equations [7]. Such studies will also require accounting for nonlinear constitutive behavior when the deformation gradients are no longer small.

Acknowledgment The authors acknowledge support from the Institute for Mathematics and its Applications at the University of Minnesota. SK also acknowledges support from the Department of Energy under award no. DE-FG02-07ER46415.

References

[1] A. Oron, S. H. Davis, and S. G. Bankoff, Long-scale evolution of thin liquid films, Rev. Mod. Phys. 63 (1997) 931.

[2] V. Gkanis and S. Kumar, Instability of creeping Couette flow past a neo-Hookean solid, Phys. Fluids 15 (2003) 2864.

[3] P. Chokshi and V. Kumaran, Weakly nonlinear analysis of viscous instability in flow past a neo-Hookean surface, Phys. Rev. E 77 (2008) 056303.

[4] V. Kumaran, G. H. Fredrickson, and P. Pincus, Flow-induced instability at the interface between a fluid and a gel at low Reynolds number, J. Phys. II France 4 (1994) 893.

[5] L. Srivatsan and V. Kumaran, Flow-induced instability at the interface between a fluid and a gel, J. Phys. II France 7 (1997) 947.

[6] S. Kumar and O. K. Matar, Dewetting of thin liquid films near soft elastomeric layers, J. Colloid Interface Sci. 273 (2004) 581.

[7] O. K. Matar, V. Gkanis, and S. Kumar, Nonlinear evolution of thin liquid films dewetting near soft elastomeric layers, J. Colloid Interface Sci. 286 (2005) 319.

[8] V. Gkanis and S. Kumar, Instability of creeping flow past a deformable wall: The role of depth-dependent modulus, Phys. Rev. E 73 (2006) 026307.

[9] R. V. Craster and O. K. Matar, Dynamics and stability of thin liquid films, Rev. Mod. Phys. 81 (2009) 1131.

[10] L. G. Leal, Advanced Transport Phenomena: Fluid Mechanics and Convective Transport Processes, Cambridge, 2007.

[11] G. Tomar, V. Shankar, S.K. Shukla, A. Sharma, and G. Biswas, Instability and dynamics of thin viscoelastic liquid films, Eur. Phys. J. E 20 (2006) 185.

[12] V. Kumaran and R. Muralikrishnan, Spontaneous growth of fluctuations in the viscous flow of a fluid past a soft interface, Phys. Rev. Lett. 84 (2000) 3310.

[13] R. Muralikrishnan and V. Kumaran, Experimental study of the instability of the viscous flow past a flexible surface, Phys. Fluids 14 (2001) 775.

[14] M. D. Eggert and S. Kumar, Observations of instability, hysteresis, and oscillation in low-Reynolds-number flow past polymer gels, J. Colloid Interface Sci. 278 (2004) 234.